Supporting Information

Laneri et al. 10.1073/pnas.1419047112

SI Text

Cohort Participants, Ethics Approval, and *Plasmodium falciparum* Case Detection and Definition

Participants. The malaria research program involving the inhabitants of the Dielmo and Ndiop villages in Senegal has been ongoing since 1990 as described and documented in detail elsewhere (1–3). Malaria transmission in Ndiop is moderate and strictly seasonal, depending upon the rainy season during the second semester. By contrast, in neighboring Dielmo, the population is exposed to intense, perennial malaria transmission, maintained during the dry season by anopheline production in a stream. The number of infectious bites per person per year, the annual entomological inoculation rate, in Dielmo is of the order of 200 (4), compared with ∼20 in Ndiop (5). This program is supported by three different institutions: the Institut Pasteur (Dakar, Senegal), the Institut de Recherche pour le Développement (IRD) (Marseille, France), and the Senegalese Ministry of Health and Prevention. An agreement between these institutions defines all research activities conducted in this program. A field research station with two dispensaries run by nurses has been constructed for the program, ensuring free-of-charge access to health care for the volunteers. Every villager can join or leave the program at any time and newborns can be included upon the request of their parents or legal guardian, therefore forming an open cohort. In the malaria research program, a family-based longitudinal study is conducted to identify all episodes of fever. Specifically for children under 15 y of age, surveillance is active with a daily visit 6 d/wk (i.e., excluding Sunday) of all of the households by field monitors to detect episodes of fever and related symptoms. In the case of suspected fever or fever-related symptoms, a thick blood smear is systematically performed. After the detailed medical examination has been completed by an experienced health worker, specific treatment is administered. When a clinical malaria attack is diagnosed, an antimalarial treatment is administered according to the National Malaria Control Program guidelines. Presence in the village of each volunteer is also recorded on a daily basis. The longitudinal surveys were approved by the Ministry of Health of Senegal and the assembled population of the two villages. Every year, the program was reexamined by the Conseil de Perfectionnement of the Institut Pasteur in Dakar and the assembled village population; informed consent of the volunteers is renewed every year. More specifically after informing them about the procedures and the purpose of the study, written informed consent was obtained from parents or guardians of children either by signature or by thumbprint on a voluntary consent form written in both French and in Wolof, the main local language. Consent was obtained in the presence of the school director, an independent witness.

***P. falciparum* Life Cycle.** The *Plasmodium* life cycle consists of multiple stages in both human and mosquito hosts. When a (female) mosquito takes a blood meal from an infected human, male and female *Plasmodium* gametocytes may be ingested. Sexual reproduction of the parasite takes place within the mosquito's stomach, forming an ookinete that penetrates the midgut wall and encysts. After a period of 10 d or so, sporozoite-stage parasites emerge from the mature oocyst and migrate to the mosquito's salivary glands. Upon a subsequent blood meal, the sporozoites invade the liver and, after a period of mitotic division, emerge into the blood, reproducing asexually in erythrocytic stages and eventually producing gametocytes to complete the cycle. Immunity to *P. falciparum* is nonsterilizing. After repeated infection, individuals may develop clinical immunity whereby they can tolerate parasites without showing symptoms. Such asymptomatic infections have blood parasite densities that are detectable in a blood smear. Antiparasite immunity, whereby individuals control parasite density, develops more slowly, but complete protection from the parasite is never achieved. Individuals with sufficient antiparasite immunity may be able to control densities below what is detectable by blood smear (although detection can be achieved by molecular methods to a lower density). Without drug treatment, an infection is estimated to last for up to 320 d (6). The model captures some key aspects of the human, parasite, and vector dynamics.

The Model

Our modeling framework was designed to be applicable to both villages. It considers both human and mosquito population variability, the first one through yearly census and the second one either directly from landing catches or indirectly estimated through the variability in local meteorological conditions, mainly local rainfall and temperature. Our model also differs from previous dynamic models applied to Ndiop (7) in that we are fitting both birth and death rates and in that we differentiate humans showing symptoms from asymptomatics (8).

The system of equations for human classes is

$$\frac{dS1}{dt}=\mu_{BS1}N+\frac{dN}{dt}-\mu_{S1E}S1+t_s\mu_T I1+\mu_{S2S1}S2-\delta S1 \qquad \textbf{[S1]}$$

$$\frac{dE}{dt}=\mu_{S1E}S1-\Phi\mu_{EI}E-(1-\Phi)\mu_{EI}E-\delta E \qquad \textbf{[S2]}$$

$$\frac{dI1}{dt}=\Phi\mu_{EI}E-(1-t_s)\mu_T I1+s_{i1}\mu_{S1E}I2+s_{i2}\mu_{S1E}S2-t_s\mu_T I1-\delta I1 \qquad \textbf{[S3]}$$

$$\frac{dI2}{dt}=(1-t_s)\mu_T I1-s_{i1}\mu_{S1E}I2+(1-\Phi)\mu_{EI}E-\mu_{I2S2}I2+s_{i3}\mu_{S1E}S2-\delta I2 \qquad \textbf{[S4]}$$

$$\frac{dS2}{dt}=\mu_{I2S2}I2-\mu_{S2S1}S2-s_{i3}\mu_{S1E}S2-s_{i2}\mu_{S1E}S2-\delta S2, \qquad \textbf{[S5]}$$

where nonlinear terms are highlighted in red and $N(t)$ is the total human population for each village at time t obtained from interpolated yearly census data as shown in Table S1.

The differential Eqs. **S1**–**S5** correspond to a large population limit of homogeneous individual-level models where each individual has exponentially distributed transition times. The birth rate $\mu_{BS1}(t)$ is set to ensure that $S1(t)+S2(t)+E(t)+I1(t)+I2(t)+R(t)=N(t)$ and the death rate was computed by fitting the data as explained in *SI Text*, *Natural Mortality Rate Estimation*).

The force of infection or transmission rate at the current time t is defined as

$$\mu_{S1E}(t)=ba^2c\int_{t_0}^{t}\frac{M(s)}{N(s)}\frac{I(s)}{N(s)}x(s)p(t-s)\,ds \qquad \textbf{[S6]}$$

with $x(s)$, the fraction of uninfected mosquitoes at a previous time s; $M(s)$, total number of mosquitoes at time s; $N(s)$, total number of humans at time s; $I(s)/N(s)$, fraction of infected humans at time s; and $p(.)$, a delay distribution that describes the mosquito

stage of the parasite life cycle and vector survival. We choose $p(.)$ to be a $\Gamma(\kappa, \tau/\kappa)$ density.

Uninfected mosquitoes become infected with malaria with a probability c when they bite (at a rate a) an infected human. The infected mosquitoes then contribute to malaria infection in humans when they again bite an uninfected human (at a rate a) and infect humans with a probability b that has information on immunity.

Instead of explicitly modeling mosquito dependence on the force of infection we can define the transmission rate μ_{S1E} at the current time t in a more general way as

$$\mu_{S1E}(t) = \int_{-\infty}^{t} \lambda(s)\gamma(t-s)d\Gamma(s), \qquad \textbf{[S7]}$$

where $\lambda(s)$ is the force of infection at a previous time s when the mosquito bites the infected human and $\gamma(t-s)$ is a delay distribution (for duration of parasite life cycle inside mosquito plus vector survival).

We take γ to be the density of a $\Gamma(\kappa, \tau/\kappa)$ random variable with mean delay τ and variance τ^2/κ.

Then

$$\gamma(t) = \frac{(\kappa/\tau)^{\kappa} t^{\kappa-1}}{(\kappa-1)!}\exp\{-\kappa t/\tau\}. \qquad \textbf{[S8]}$$

To implement the multiiterated filtering methodology it is necessary to transform the non-Markovian integral **[S7]** in a Markovian chain of differential equations. We consider delay distributions leading to finite-dimensional Markovian representations. The consideration of Gamma-distributed transitions between the latent $\lambda(t)$ and current $\mu_{S1E}(t)$ force of infection replaces the integral and the development–mortality kernel of Eq. **S7** with a series of compartments between μ_{EI} and λ following refs. 9 and 10). We replace the integral **[S7]** by the κ-dimensional Markovian system, $\lambda(t), \ldots \lambda_{\kappa-1}(t), \lambda_{\kappa}(\equiv \mu_{S1E}(t))$:

$$\frac{\lambda_1}{dt} = (\lambda - \lambda_1)\frac{\kappa}{\tau}, \qquad \textbf{[S9]}$$

$$\frac{\lambda_i}{dt} = (\lambda_{i-1} - \lambda_i)\frac{\kappa}{\tau} \quad \text{for } i = 2, \ldots, \kappa-1, \qquad \textbf{[S10]}$$

$$\frac{\mu_{S1E}}{dt} = (\lambda_{\kappa-1} - \mu_{S1E})\frac{\kappa}{\tau}. \qquad \textbf{[S11]}$$

The differential Eqs. **S9–S11** correspond to Gamma-distributed transitions for the latent period of the force of infection. Therefore, Eqs. **S1–S5** for the human population and Eqs. **S9–S11** for the mosquito populations completely determine our coupled human–mosquito malaria model. After experimenting with different choices of κ, we fixed $\kappa = 3$.

Transmission and the Entomological Inoculation Rate

The entomological inoculation rate (EIR) is the number of infectious bites per person per unit time. It can be defined as the product of the human biting rate ($M(t)\,a$) and the sporozoite rate (S).

$$\mathrm{EIR}(t) = M(t)a\,S. \qquad \textbf{[S12]}$$

The human biting rate is the number of bites per human per unit time, where $M(t)$ equals the number of *Anopheles* per person at a given time and a equals the average number of persons bitten by one *Anopheles* in 1 d. The sporozoite rate (S) is the proportion of female mosquitoes containing infective-stage parasites in their salivary glands upon dissection and therefore infectious. Within our framework we could rewrite λ in Eq. **S7** by comparing it with Eq. **S6** as

$$\lambda(t) = \left[\frac{I1(t) + q_f \times I2(t) + s_f \times S2(t)}{N(t)}\exp\{\mathrm{EIR}(t) + D(t)\}\frac{d\Gamma}{dt}\right]\overline{\beta}, \qquad \textbf{[S13]}$$

with $\overline{\beta}$ a dimensional constant set as $\overline{\beta} = yr^{-1}$, which is required to give $\mu_{S1E}(t)$ units of y^{-1}.

Here, q_f and s_f are the fractions of asymptomatics in classes $I2$ and $S2$ respectively capable of infecting mosquitoes, with the fraction of infectives from $I1$ set to 1 for comparison.

Environmental noise was included as multiplicative Gamma noise to take into account the stochasticity that arises from variations in vector abundance and behavior (11, 12). $\Gamma(t)$ denotes a Gamma process with stationary independent increments such that $\Gamma(t) - \Gamma(s) \sim \Gamma([t-s]/\sigma^2, \sigma^2)$, where $\Gamma(a, b)$ is the Gamma distribution with mean ab and variance ab^2. The rationale behind choosing a Gamma noise is that of keeping the term $\lambda(t)$ positive at all times; because a Gamma process is increasing, its derivative ($d\Gamma/dt$) is nonnegative at all times. For the continuous-time process in **[S1–S5]** and **[S9–S11]**, all of the states are necessarily nonnegative. When discretizing to give a Euler solution with time step Δ, this property could be violated. However, with $\Delta = 1$ d, such potential numerical issues did not cause problems in our fitted models.

We modeled drug treatment as a rectangular window function D that is equal to one for the time period of the corresponding drug treatment and zero otherwise. Different drug treatment periods were taken from the dataset:

$$D(t) = \beta_{\mathrm{qui}} D\left[t_{\mathrm{qui}}\right] + \beta_{\mathrm{clo}} D[t_{\mathrm{clo}}] + \beta_{\mathrm{fan}} D\left[t_{\mathrm{fan}}\right] + \beta_{\mathrm{act}} D[t_{\mathrm{act}}]. \qquad \textbf{[S14]}$$

Throughout the text, we refer to this model as the EIR transmission model. The timing of transmission is well emulated by the EIR model for both Dielmo and Ndiop, although not the intensity, a fact that could be due to spatial heterogeneities not taken into account in our model.

Transmission and Climatic Variables

We expect mosquito population $M(s)$ in Eq. **S6** to be seasonal, to have a dependence on climatic factors, and to have a random component. We can rewrite the transmission λ in Eq. **S6** as

$$\lambda(t) = \left[\frac{I1(t) + q_f \times I2(t) + s_f \times S2(t)}{N(t)} \times \exp\left\{\sum_{i=1}^{k}\beta_i s_i(t) + Z(t) + D(t)\right\}\frac{d\Gamma}{dt}\right]\overline{\beta}, \qquad \textbf{[S15]}$$

where $\overline{\beta}$ is a dimensional constant and we set $\overline{\beta} = \mathrm{y}^{-1}$. Here, time is measured in units of years.

Seasonality is modeled nonparametrically through the coefficients $\{\beta_i\}$ of a periodic cubic B-spline basis $s_i(t), i = 1, \ldots, 6$ constructed using six evenly spaced knots. It represents interannual variability in transmission and was modeled by

$$\log \beta_{\mathrm{seas}}(t) = \sum_{i=0}^{5} b_i s_i(t), \qquad \textbf{[S16]}$$

where $s_i(t)$ is a periodic cubic B-spline basis defined so that $s_i(t)$ has a maximum at $t = (2i+1)/12$, and normalized so that $\sum_{i=0}^{5} s_i(t) = 1$. When only splines were considered, we called the model the Sp model.

Time-varying covariates enter via the vector $Z(t)$. Temperature and rainfall variability lead to air and soil moisture fluctuations that drive changes in mosquito population densities and, for temperature, may alter the rate of development of the parasite within the mosquito. In this direction we suggested a (simplest parsimonious) linear combination of temperature and rainfall as an indicator of humidity conditions (SpTR model) as

$$Z(t) = \beta_{\text{rain}} R(t) + \beta_{\text{temp}} T(t), \qquad \textbf{[S17]}$$

where $R(t)$ is the standardized rainfall anomaly and $T(t)$ is the standardized temperature anomaly. All of the climate covariates were normalized to zero mean and unit variance. Therefore, in this model rainfall forcing is represented by the term $\beta_{\text{rain}} R(t)$ and temperature forcing is represented by the term $\beta_{\text{temp}} T(t)$.

The link of the malaria vector breeding sites to land water content (LWC) and/or soil moisture (SM) states in an area has been reported extensively in the past (13). For regions in the world where direct estimates of the local LWC or SM values are lacking, the construction of analogs from rainfall and temperature is justified (14). Soil moisture plays an important role in hydrological processes with partitioning of rainfall into infiltration and runoff or partitioning of net radiation into sensible and latent heat and as such, acting as an analog of the water content remaining in the soil after precipitation. Thus, the combined effect of precipitation and evaporation on SM can be defined as R_k/ET_j with $j = 1, \ldots, k$, where R_k is precipitation of k days ago, and ET_j is evaporation of j days ago. As such, land surface soil moisture integrates the local precipitation and surface evaporation that in subtropical regions is largely dependent on temperature (14). It is well known that there exists a negative correlation between SM states and mean and maximum temperatures, more so in the subtropics and semidesertic areas (15, 16). Eltahir and collaborators (17) also suggested a link between rainfall and surface wet bulb temperature during summer months in the United States, with wet bulb temperature being an indicator of soil moisture (18). Based on these facts we propose an alternative transmission model (SpROT) with an additional term representing the interaction between rainfall and temperature:

$$Z(t) = \beta_{\text{rain}} R(t) + \beta_{\text{temp}} T(t) + \beta_{\text{ROT}} \frac{R(t)}{T(t)}. \qquad \textbf{[S18]}$$

Therefore, the soil moisture term is represented by $\beta_{\text{ROT}} R(t)/T(t)$.

Rainfall time series from Dielmo (13,685662N, 16,38463W) and Ndiop (13,724620N, 16,409324W) come from a meteorological ground-based manually operated station in each village (Fig. S3).

Due to the lack of complete local village data, we averaged the temperature series extracted from the four nearest towns [e.g., Cap Skirring, Kaolack, Diourbel, and Ziguinchor; National Oceanic and Atmospheric Administration (NOAA) National Climate Data Center (NCDC) Global Hydrology and Climatology Network (GHCN) v2] (19). Cap Skirring and Ziguinchor are in Casamance near the border with Guinée Bissau. Diourbel is east of Dakar, in the Sahel region, and Kaolack is the closest town to Dielmo, in between other stations. Maximum, mean, and minimum averaged temperature time series are shown in Fig. S4.

Drug treatment was included as in the previous section through Eq. **S14**.

As described in the main text, the rate of change of the force of infection μ_{S1E} is driven by an exogenous forcing including three sources of variability that influence the vector's abundance and behavior, i.e., seasonality, climate covariates (here, rainfall and temperature), and random noise.

Immunity and Recovery Rates. The rate of loss of immunity from asymptomatics $I2$ to subpatent $S2$ was modeled as dependent on transmission (8, 20, 21),

$$\mu_{I2S2}(t) = \frac{\mu_{S1E}(t)}{e^{\mu_{S1E}(t) t_{I2S2}} - 1},$$

with t_{I2S2} a characteristic time for the transition in the sense that $1/t_{I2S2}$ is the basal rate at which transmission tends to zero. Therefore, t_{I2S2} is expected to be longer in Ndiop than in Dielmo, given the evidence of higher parasite immunity in Dielmo. According to this formulation immunity lasts until the occurrence of a gap of t_{I2S2} mo without exposure. This function is consistent with the fact that in high-transmission places like Dielmo (high μ_{S1E}) the decay of immunity is slower (μ_{I2S2} will be smaller) than in low unstable-transmission sites like Ndiop. Similarly, clearance of subpatent infections was modeled as (20)

$$\mu_{S2S1}(t) = \frac{\mu_{S1E}(t)}{e^{\mu_{S1E}(t) t_{S2S1}} - 1}.$$

This function is consistent with the fact that in high-transmission places like Dielmo (high μ_{S1E}) the process of full recovery is slower than in low unstable-transmission sites like Ndiop.

Superinfection and Recrudescence of Existing Infections. Reinfection from asymptomatic class $I2$ to infected symptomatic $I1$ was considered as a fraction of the force of infection:

$$\mu_{I2I1} = si_1 \mu_{S1E}.$$

This transition takes into account new infections, i.e., superinfection, as well as recrudescent infections. According to our modeling results, even that the fraction of force of infection (relative to that needed to pass from susceptible to exposed) needed for an individual to pass from asymptomatic to symptomatic was much smaller for Dielmo ($si_1 \approx 0.02$) than for Ndiop ($si_1 \approx 0.1$), the forces needed to go from $I2$ to $I1$ are comparable for both villages. This is because the overall force of infection is 10 times higher in Dielmo than in Ndiop.

Superinfection from subpatent infections $S2$ to symptomatic $I1$ was considered as

$$\mu_{S2I1} = si_2 \mu_{S1E}.$$

This transition denotes mainly superinfection in the sense that humans with ultralow parasite densities flip to the symptomatic state.

Reinfection from class $S2$ to class $I2$ was considered as

$$\mu_{S2I2} = si_3 \mu_{S1E}.$$

Our results indicate that the fraction of the force of infection (relative to that needed to pass from susceptible to exposed) resulting in change of state from subpatent to asymptomatic is the same for both villages (0.5); however, as the overall force of infection is 10 times higher in Dielmo than in Ndiop, the total force needed to go from $S2$ to $I2$ is 10 times higher in Dielmo than in Ndiop.

Observation Model. Let C_n be the number of people moving from class E, $S2$, or $I2$ to class $I1$ between time t_{n-1} and t_n, where t_n is the nth observation time; i.e.,

$$C_n = \int_{t_{n-1}}^{t_n} (dN_{EI1}(s) + dN_{S2I1}(s) + dN_{I2I1}(s)).$$

Observations Y_n at time t_n are then modeled as $Y_n | C_n \sim \text{Negbin}(\text{mean} = \rho C_n, \text{var} = \rho C_n + \rho^2 \sigma_{\text{obs}}^2 C_n^2)$. Here ρ is a number

between 0 and 1 that corresponds to the fraction of the infected symptomatic population that reports to the hospital. In our case ρ is expected to be equal to one given that every fever case is diagnosed and, if confirmed, is treated. This fraction was fitted and the obtained values were $\approx$ 0.9 (Tables S3 and S4). The negative binomial distribution accounts for the possibility of overdispersion.

Natural Mortality Rate Estimation

Assuming a population in demographic equilibrium [$\rho_h(\alpha)$ time independent] and ignoring extra mortality due to disease, we can define the density of people ρ_h at a given age α as

$$\rho_h(\alpha) = \delta \frac{e^{-\delta\alpha}}{1 - e^{-\delta\alpha_m}}, \quad \text{[S19]}$$

with δ the natural mortality rate and α_m the maximum age in the human population. Fitted values for the natural mortality rate are shown in Fig. S1 and were set as the fixed value for mortality in the models (i.e., 0.03 1/y).

Population Changes

During the rainy season there is a general return to the village because adolescents and adults return home to help with the harvest. Additionally, is it the holiday period and thus certain children will also return to the village (e.g., those having gone to Koranic school or accompanied adults to towns/cities). In Fig. S5 we compare occupation for both villages during the first (January–June) and second (July–December) semesters of the year. The graph shows the total number of days present cumulative for all villagers during the semester–year for both villages. We see that occupation for both villages does not vary significantly. Although there is a small semestrial increase in the population present in the villages, this is not significant for the overall population or for the child population, which contributes the major part of the clinical episodes. Given that not a clear pattern was observed, this variable was not included in model transmission.

Since the introduction of the on-site medical facility, there has been no mortality due to malaria. Obviously there have been other causes of mortality. The populations are typical of those living in rural malaria endemic regions with (previously) no access to health care. There are no intervillage differences, because living so close (a few kilometers), there is interaction. The only significant behavioral change followed the introduction of bed nets after 2008. There are intraannual population differences but these are small.

Fitted Parameters

We carried out all numerical simulations in the R computing environment, using the R package Pomp (22) to implement the algorithm for statistical inference, which is detailed elsewhere (23, 24). Errors were calculated as a weighted average of all of the fits obtained. The weight assigned to each fit was defined as the normalized likelihood of the fit.

Sensitivity Analysis. To explore the sensitivity of the results to our compound of rainfall and temperature, we also fitted the malaria time series with transmission modeled using temperature and rainfall as separate covariates. We recall here the goodness of fit when taking into account contributions both of rainfall and of temperature in transmission from Tables S3 and S4 (Dielmo, loglik = −782, AIC_c = 1,642; Ndiop, loglik = −631, AIC_c = 1,344). With the combination of splines and temperature (Dielmo, loglik = −784, AIC_c = 1,643; Ndiop, loglik = −634, AIC_c = 1,347) the goodness of fit gets worse than when both contributions are taken into account in transmission. The same happens when a combination of splines and rainfall is considered (Dielmo, loglik = −785, AIC_c = 1,645; Ndiop, loglik = −632, AIC_c = 1,344). Interestingly for the case of Ndiop, accounting for the temperature covariate does not improve significantly the goodness of fit, whereas it does in the case of Dielmo. Rainfall consideration, however, seems to be more crucial to reproduce malaria dynamics in both villages.

Fitting the Malaria Model by Maximum Likelihood. Fitting partially observed nonlinear stochastic dynamic models to data is a methodological challenge. We estimated parameters with a recently developed method, iterated filtering, that allows the likelihood-based comparison of models of disease transmission. This methodology has a plug-and-play property (11, 12), meaning that one needs only to numerically simulate the differential equations that define the model. This enables comparison among a wide class of models. An overview of an iterated filtering procedure, which converges to the maximum of the likelihood function (25, 26), is presented elsewhere (24) where the computationally challenging step is an application of widely used sequential Monte Carlo techniques (27, 28). The method consists of two loops, with the external loop essentially iterating an internal, "filtering" loop and in so doing generating a new, improved estimate of the parameter values at each iteration. The filtering loop implements a selection process for a large number of "particles" over time. For each time step, a particle can be seen as a simulation characterized by its own set of parameter values. Particles can survive or die as the result of a resampling process, with probabilities determined by their likelihood given the data. From this selection process over the whole extent of the data, a new estimate of the parameters is generated, and from this estimate, a cloud of new particles is reinitialized using a given noise intensity adjusted by a cooling factor. This noise, as well as the stochasticity of the dynamics of the system itself, provides the variability for the selection process of the particles to act upon. Further details can be found in refs. 22, 25, and 27–29. Given the huge amount of simulations needed, these computations were done using a cluster for high-performance computing. Fits for Dielmo and Ndiop are shown in Figs. S6 and S7.

1. Trape JF, et al. (1994) The Dielmo project: A longitudinal study of natural malaria infection and the mechanisms of protective immunity in a community living in a holoendemic area of Senegal. *Am J Trop Med Hyg* 51(2):123–137.
2. Rogier C, et al. (1999) *Plasmodium falciparum* clinical malaria: Lessons from longitudinal studies in Senegal. *Parassitologia* 41(1–3):255–259.
3. Trape JF, et al. (2011) Malaria morbidity and pyrethroid resistance after the introduction of insecticide-treated bednets and artemisinin-based combination therapies: A longitudinal study. *Lancet Infect Dis* 11(12):925–932.
4. Fontenille D, et al. (1997) High annual and seasonal variations in malaria transmission by anophelines and vector species composition in Dielmo, a holoendemic area in Senegal. *Am J Trop Med Hyg* 56(3):247–253.
5. Fontenille D, et al. (1997) Four years' entomological study of the transmission of seasonal malaria in Senegal and the bionomics of *Anopheles gambiae* and *A. arabiensis*. *Trans R Soc Trop Med Hyg* 91(6):647–652.
6. Felger I, et al. (2012) The dynamics of natural *Plasmodium falciparum* infections. *PLoS ONE* 7(9):e45542.
7. Cancré N, et al. (2000) Bayesian analysis of an epidemiologic model of *Plasmodium falciparum* malaria infection in Ndiop, Senegal. *Am J Epidemiol* 152(8):760–770.
8. Filipe JAN, Riley EM, Drakeley CJ, Sutherland CJ, Ghani AC (2007) Determination of the processes driving the acquisition of immunity to malaria using a mathematical transmission model. *PLoS Comput Biol* 3(12):e255.
9. Wearing HJ, Rohani P, Keeling MJ (2005) Appropriate models for the management of infectious diseases. *PLoS Med* 2(7):e174.
10. Lloyd AL (2001) Realistic distributions of infectious periods in epidemic models: Changing patterns of persistence and dynamics. *Theor Popul Biol* 60(1):59–71.
11. Bretó C, He D, Ionides EL, King AA (2009) Time series analysis via mechanistic models. *Ann Appl Stat* 3:319–348.
12. He D, Ionides EL, King AA (2010) Plug-and-play inference for disease dynamics: Measles in large and small populations as a case study. *J R Soc Interface* 7(43):271–283.
13. Manguin S, Carnevale P, Mouchet J (2008) *Biodiversity of Malaria in the World* (John Libbey Eurotext, Montrouge, Ile de France, France).
14. Shang KZ, et al. (2007) A scheme for calculating soil moisture content. *Atmos Chem Phys* 7:5197–5206.
15. Karl T (1986) The relationship of soil moisture parameterization to subsequent seasonal and monthly mean temperature in the US. *Bull Am Meteorol Soc* 114: 675–686.

16. Georgakakos K, Bae D, Cayan D (1995) Hydroclimatology of continental watersheds, 1: Temporal analysis. *Water Resour Res* 31(3):655–675.
17. Eltahir E, Pal J (1996) Relationship between surface conditions and subsequent rainfall in convective storms. *J Geophys Res* 101:26337–26345.
18. Findell K, Eltahir E (1997) An analysis of the soil moisture-rainfall feedback, based on direct observations from Illinois. *Water Resour Res* 33:725–735.
19. Peterson TC, Russell SV (1997) An overview of the Global Historical Climatology Network temperature data base. *Bull Am Meteorol Soc* 78:2837–2849.
20. Alonso D, Bouma MJ, Pascual M (2011) Epidemic malaria and warmer temperatures in recent decades in an East African highland. *Proc Biol Sci* 278(1712):1661–1669.
21. Aron JL (1988) Mathematical-modeling of immunity to malaria. *Math Biosci* 90: 385–396.
22. King AA, et al. (2010) *Pomp: Statistical Inference for Partially Observed Markov Processes (R Package) Version 0.43-1* (R Foundation for Statistical Computing, Vienna). Available at pomp.r-forge.r-project.org. Accessed June 5, 2015.
23. Laneri K, et al. (2010) Forcing versus feedback: Epidemic malaria and monsoon rains in northwest India. *PLoS Comput Biol* 6(9):e1000898.
24. Bhadra A, et al. (2011) Malaria in Northwest India: Data analysis via partially observed stochastic differential equation models driven by Lévy noise. *J Am Stat Assoc* 106:440–451.
25. Ionides EL, Bretó C, King AA (2006) Inference for nonlinear dynamical systems. *Proc Natl Acad Sci USA* 103(49):18438–18443.
26. Ionides EL, Bhadra A, Atchadé Y, King AA (2011) Iterated filtering. *Ann Stat* 39: 1776–1802.
27. Doucet A, de Freitas N, Gordon NJ, eds (2001) *Sequential Monte Carlo Methods in Practice* (Springer, New York).
28. Cappé O, Godsill S, Moulines E (2007) An overview of existing methods and recent advances in sequential Monte Carlo. *Proc IEEE* 95:899–924.
29. King AA, Ionides EL, Pascual M, Bouma MJ (2008) Inapparent infections and cholera dynamics. *Nature* 454(7206):877–880.

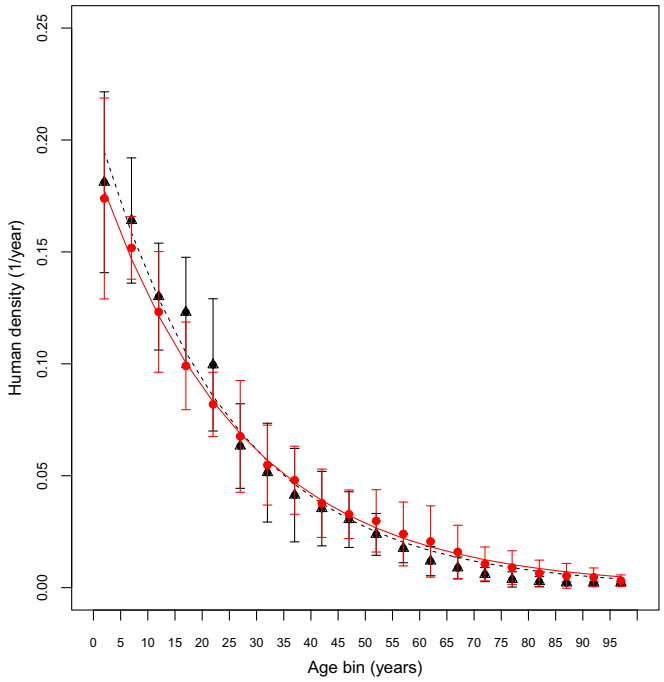

Fig. S1. Age structure and natural mortality rate for Dielmo (red) and Ndiop (black). The average population for each age bin was taken over 15 y for Ndiop (black triangles) and 18 y for Dielmo (red circles); error bars are twice the SD of the mean during those years. Natural mortality rate for Dielmo and Ndiop was fitted according to Eq. **S19**. Fitted values are $\delta = 0.0371/\text{y}$ for Dielmo (red solid line) and $\delta = 0.0411/\text{y}$ for Ndiop (black dotted line).

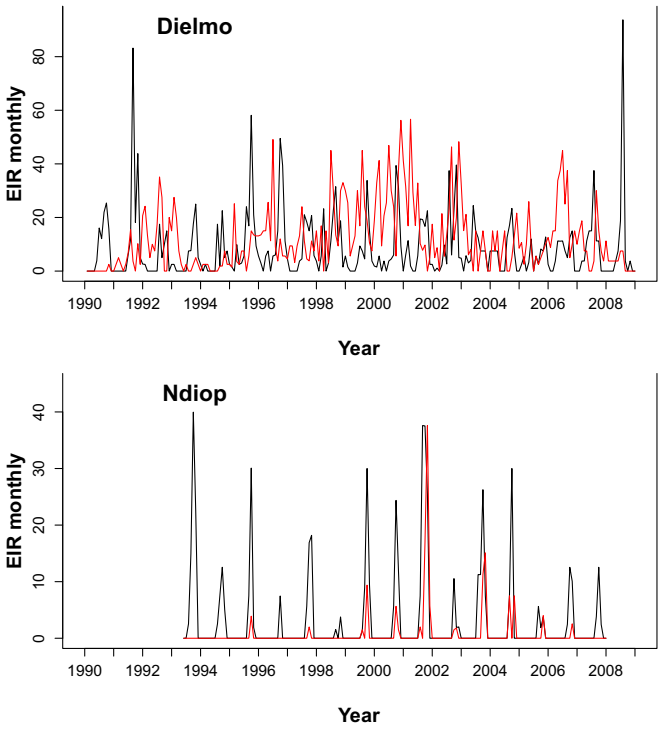

Fig. S2. Monthly entomological inoculation rate (EIR) by mosquito species for Dielmo (*Upper*) and Ndiop (*Lower*). Red lines, *A. funestus*; black lines, *A. gambiae s.l.*

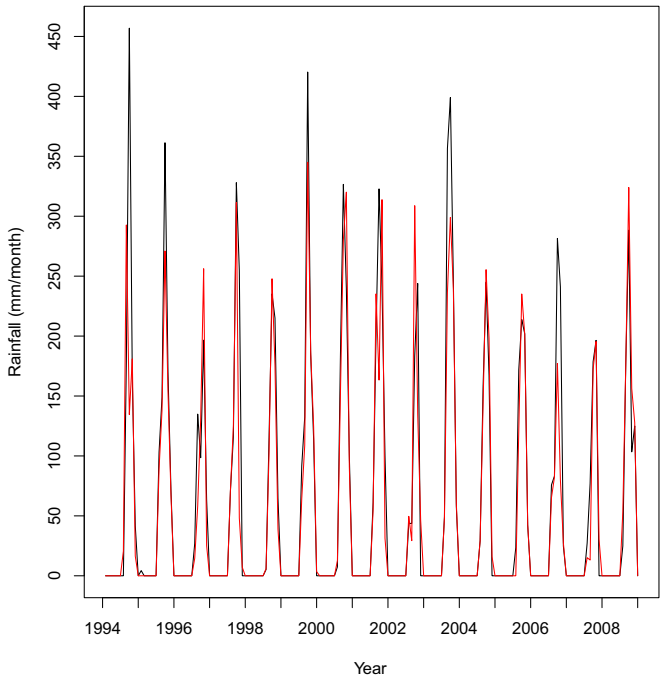

Fig. S3. Monthly rainfall for Ndiop (black) and Dielmo (red). Note the high similarity between rainfall in the two villages.

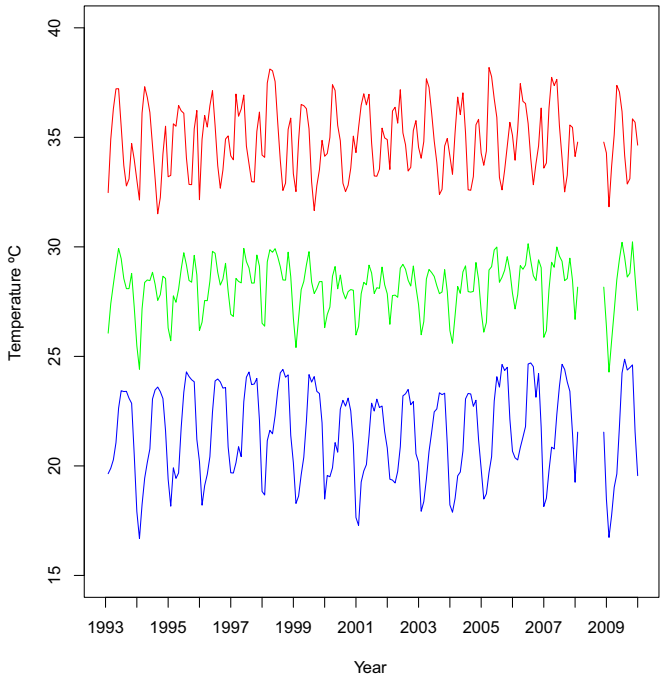

Fig. S4. Maximum (red), mean (green), and minimum (blue) temperature averaged over four locations: Diourbel, Kaolack, Cap Skirring, Ziguinchor. Temperature was extracted from NOAA NCDC GHCN v2 (19).

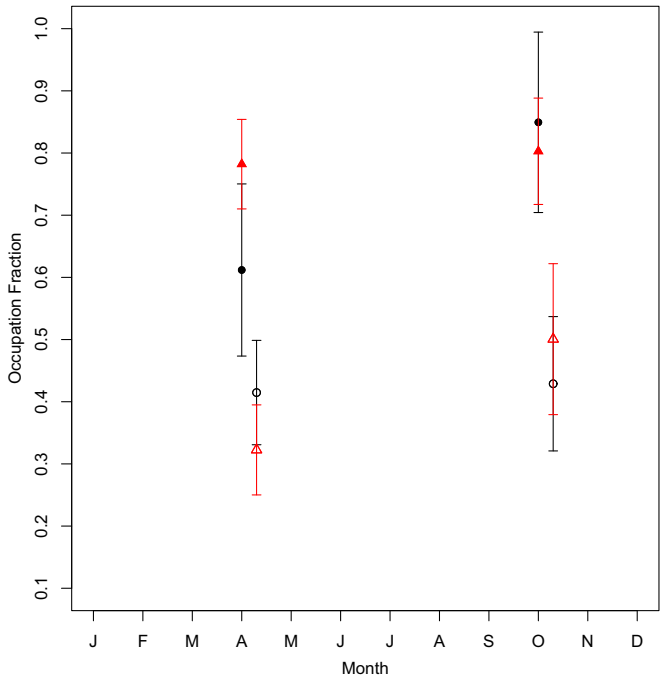

Fig. S5. Occupation fraction for Dielmo (red triangles) and Ndiop (black circles). Solid symbols correspond to all of the population and open symbols correspond to children (less than 15 y old). Mean occupation was calculated as mean number of days present in the village by person during the whole semester. Error bars are the SD of the mean for the 19 y in Dielmo and the 16 y in Ndiop. Mean occupation and error bars are centered on the corresponding semester; they are plotted slightly displaced for clarity.

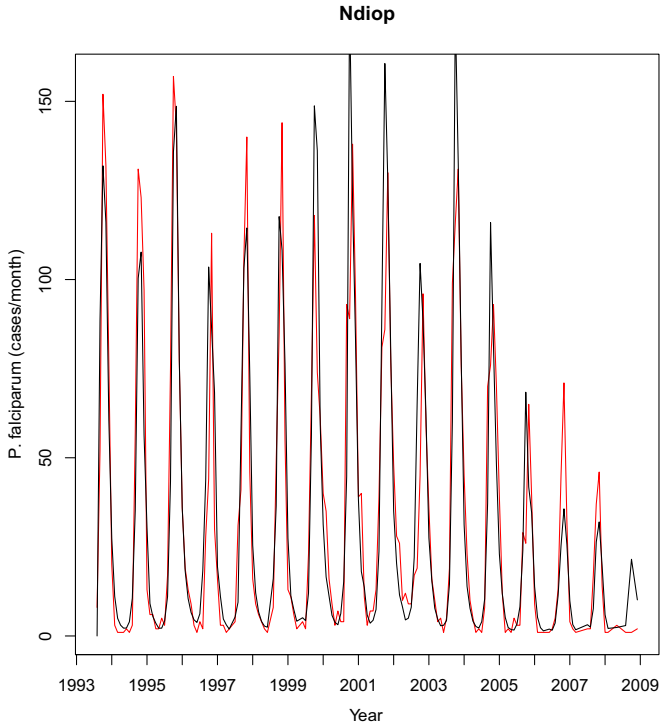

Fig. S6. Ndiop *P. falciparum* time series fitted by multiiterated filtering (MIF) procedure. Transmission was modeled by taking into account different drug periods, seasonal variability, and local climate variability. Population variability was also considered. Model: spTR. Data are shown in red and fit in black.

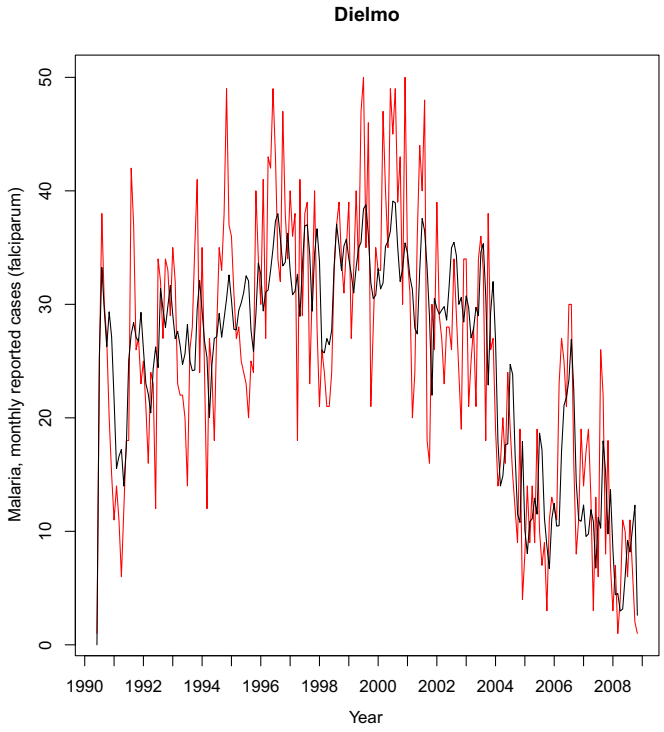

Fig. S7. Dielmo *P. falciparum* time series fitted by multiiterated filtering (MIF) procedure. Transmission was modeled by taking into account different drug periods, seasonal variability, and local climate variability. Population variability was also considered. Model: SpTR. Data are shown in red and fit in black.

Table S1. Population (number of inhabitants) of Ndiop and Dielmo

Village	1990	1991	1992	1993	1994	1995	1996	1997	1998	1999	2000	2001	2002	2003	2004	2005	2006	2007	2008
Dielmo	290	301	303	321	335	333	381	363	434	434	446	414	397	401	405	460	456	487	508
Ndiop	—	—	—	416	414	444	417	476	604	528	513	471	498	455	422	549	477	528	508

Table S2. List of symbols for the malaria model

Symbol	Description	Unit	Estimated? Y/N	Constraints
μ_{XY}	Per-capita rate of transition from compartment X to Y; X, $Y \in \{S1, E, I1, I2, S2\}$	y^{-1}	Y	>0
β_i	Ith spline coefficient	—	Y	None
$\overline{\beta}$	Dimensionality constant	y^{-1}	N	1
τ	Mean development delay for mosquitoes	d	N	11
σ	SD of the process noise	$y^{1/2}$	Y	>0
ρ	Reporting fraction of people in the transition from E to $I1$	—	Y	[0–1]
Δ	Time step for stochastic Euler integration	d	N	1
δ	Natural mortality rate	1/y	N	0.03
σ_{obs}	SD of the observation noise	—	Y	>0
X_0	Initial fraction of people in compartment X; $X \in \{S1, E, I1, I2, S2\}$	—	Y	[0–1]
q_f	Infectivity of asymptomatic people	—	Y	[0–1]
s_f	Infectivity of subpatent infected people	—	Y	[0–1]
ps	Probability of becoming a symptomatic case	—	Y	[0–1]
ts	Fraction of successful treatments	—	Y	[0–1]
si_1	Fraction of force of infection for superinfection (from $I2$ to $I1$)	—	Y	[0–1]
si_2	Fraction of force of infection for superinfection (from $S2$ to $I1$)	—	Y	[0–1]
si_3	Fraction of force of infection for superinfection (from $S2$ to $I2$)	—	Y	[0–1]
β_{rain}	Rainfall coefficient in transmission	—	Y	None
β_{temp}	Temperature coefficient in transmission	—	Y	None
β_{ROT}	Rainfall over temperature coefficient in transmission	—	Y	None
β_{EIR}	Entomological inoculation rate coefficient in transmission	—	Y	>0

Fixed parameters are $\overline{\beta} = 1\ y^{-1}$, $n_\lambda = 2$, $\Delta = 1$ d, $\delta = 0.03\ y^{-1}$, and $ft = 1$.

Table S3. Fitted parameters for Dielmo with transmission modeled as proportional to EIR, with splines, temperature, and rainfall anomalies (SpTR) and with the additional rain over temperature (ROT) term

Description	Symbol	Unit	Dielmo, EIR	Dielmo, SpTR	Dielmo, SpROT
Likelihood	Loglik	—	−800	−782	−783
No. data points	n	—	221	221	221
No. free parameters	p	—	26	33	34
Second-order or corrected Akaike information criteria	AIC_c	—	1,659	1,642	1,646
Time from exposed to infected	$1/\mu_{EI}$	d	15_{1}	13_{4}	13_{3}
Time from symptomatic to asymptomatic	t_{I1I2}	d	146_{36}	109_{30}	109_{15}
Time of immunity decay from asymptomatic to subpatent	t_{I2S2}	d	36_{15}	36_{10}	51_{1}
Time of recovery after treatment	t_{I1S1T}	d	10_{1}	10_{1}	11_{1}
Time of recovery from subpatent infection to susceptible	t_{S2S1}	d	11_{1}	9_{1}	8_{1}
Development time of parasite	τ	d	11	11	11
Measurement noise	σ	—	$0.14_{0.01}$	$0.13_{0.01}$	$0.15_{0.01}$
Observation noise	σ_{obs}	—	$0.02_{0.01}$	$0.03_{0.01}$	$0.04_{0.01}$
Infectivity of *I*2 class	q_f	—	$0.9_{0.1}$	$0.7_{0.1}$	$0.7_{0.1}$
Infectivity of *S*2 class	s_f	—	$0.6_{0.1}$	$0.5_{0.1}$	$0.5_{0.1}$
Reporting rate	ρ	—	$0.98_{0.01}$	$0.99_{0.01}$	$0.99_{0.01}$
Probability of developing symptoms	ps	—	$0.08_{0.01}$	$0.04_{0.02}$	$0.04_{0.01}$
Initial susceptible population	*S*1.0	—	$0.07_{0.01}$	$0.09_{0.04}$	$0.1_{0.2}$
Initial exposed population	*E*.0	—	$0.4_{0.3}$	$0.1_{0.1}$	$0.2_{0.3}$
Initial infected symptomatic population	*I*1.0	—	$0.1_{0.2}$	$0.06_{0.06}$	$0.3_{0.3}$
Initial infected asymptomatic population	*I*2.0	—	$0.4_{0.3}$	$0.09_{0.09}$	$0.4_{0.3}$
Initial susceptible subpatent population	*S*2.0	—	$0.05_{0.05}$	$0.003_{0.003}$	$0.04_{0.1}$
Superinfection fraction, from *I*2 to *I*1	si_1	—	$0.02_{0.01}$	$0.02_{0.01}$	$0.02_{0.01}$
Superinfection fraction, from *S*2 to *I*1	si_2	—	$0.87_{0.1}$	$0.85_{0.01}$	$0.9_{0.01}$
Superinfection fraction, from *S*2 to *I*2	si_3	—	$0.56_{0.1}$	$0.53_{0.01}$	$0.60_{0.05}$
Treatment success	ts	—	$0.94_{0.01}$	$0.91_{0.02}$	$0.91_{0.02}$
EIR coefficient	β_{EIR}	—	$-0.009_{0.001}$	—	—
Rainfall coefficient	β_{rain}	—	—	$-0.07_{0.01}$	$-0.2_{0.08}$
Temperature coefficient	β_{temp}	—	—	$-0.04_{0.01}$	$-0.1_{0.02}$
R over *T* coefficient	β_{ROT}	—	—	—	$0.16_{0.03}$
Drug coefficient Quinine	β_{qui}	—	$1.04_{0.01}$	1.09_{1}	$0.9_{0.1}$
Drug coefficient Chloroquine	β_{clo}	—	$2.9_{0.4}$	2.98_{4}	$3_{0.2}$
Drug coefficient Fansidar	β_{fan}	—	$-0.25_{0.02}$	$-0.19_{0.01}$	$-0.1_{0.01}$
Drug coefficient ACT	β_{act}	—	$-1.27_{0.03}$	$-1.41_{0.02}$	$-1.5_{0.2}$
Spline coefficient	β_1	—	—	$3.3_{0.2}$	$2.2_{0.2}$
Spline coefficient	β_2	—	—	$1.96_{0.02}$	$1.8_{0.2}$
Spline coefficient	β_3	—	—	$1.6_{0.1}$	$1.7_{0.1}$
Spline coefficient	β_4	—	—	$2.72_{0.3}$	$2.8_{0.2}$
Spline coefficient	β_5	—	—	$0.96_{0.02}$	$0.7_{0.1}$
Spline coefficient	β_6	—	—	$2.52_{0.03}$	$2.6_{0.2}$

The number of fitted parameters, including initial conditions, and data points are listed. According to the second-order or corrected Akaike information criteria (AIC_c), the SpTR model better fits the observed data. Subscript numbers are the errors of the fitted parameters.

Table S4. Fitted parameters for Ndiop with transmission modeled as proportional to EIR, with splines, temperature, and rainfall anomalies (SpTR) and with the additional rain over temperature (ROT) term

Description	Symbol	Unit	Ndiop, EIR	Ndiop, SpTR	Ndiop, SpROT
Likelihood	Loglik	—	−737	−631	−631
No. data points	n	—	172	172	172
No. free parameters	p	—	26	33	34
Second-order Akaike information criteria	AIC_c	—	1536	1344	1347
Time from exposed to infected	$1/\mu_{EI}$	d	10_{1}	9_{1}	9_{1}
Time from symptomatic to asymptomatic	t_{I1I2}	d	98_{1}	146_{30}	106_{109}
Time of immunity decay from asymptomatic to subpatent	t_{I2S2}	d	120_{30}	109_{30}	91_{25}
Time of recovery after treatment	t_{I1S1T}	d	31_{6}	11_{1}	11_{1}
Time of recovery from subpatent infection to susceptible	t_{S2S1}	d	109_{30}	109_{30}	109_{33}
Development time of parasite	τ	d	11	11	11
Measurement noise	σ	—	$0.25_{0.02}$	$0.25_{0.02}$	$0.18_{0.01}$
Observation noise	σ_{obs}	—	$0.15_{0.05}$	$0.15_{0.05}$	$0.05_{0.03}$
Infectivity of *I*2 class	q_f	—	$0.6_{0.2}$	$0.5_{0.2}$	$0.7_{0.1}$
Infectivity of *S*2 class	s_f	—	$0.9_{0.2}$	$0.5_{0.2}$	$0.6_{0.1}$
Reporting rate	ρ	—	$0.99_{0.01}$	$0.98_{0.01}$	$0.99_{0.01}$
Probability of developing symptoms	ps	—	$0.6_{0.2}$	$0.8_{0.1}$	$0.7_{0.1}$
Initial susceptible population	*S*1.0	—	$0.3_{0.2}$	$0.7_{0.2}$	$0.7_{0.2}$
Initial exposed population	*E*.0	—	$0.08_{0.02}$	$0.03_{0.02}$	$0.03_{0.02}$
Initial infected symptomatic population	*I*1.0	—	$0.3_{0.01}$	$0.3_{0.3}$	$0.3_{0.2}$
Initial infected asymptomatic population	*I*2.0	—	$0.08_{0.02}$	$0.01_{0.01}$	$0.1_{0.1}$
Initial susceptible subpatent population	*S*2.0	—	$0.3_{0.02}$	$0.02_{0.05}$	$0.04_{0.07}$
Superinfection fraction, from *I*2 to *I*1	si_1	—	$0.7_{0.02}$	$0.1_{0.1}$	$0.14_{0.04}$
Superinfection fraction, from *S*2 to *I*1	si_2	—	$0.1_{0.1}$	$0.4_{0.1}$	$0.5_{0.1}$
Superinfection fraction, from *S*2 to *I*2	si_3	—	$0.1_{0.1}$	$0.5_{0.1}$	$0.6_{0.1}$
Treatment success	ts	—	$0.89_{0.03}$	$0.92_{0.03}$	$0.91_{0.04}$
EIR coefficient	β_{EIR}	—	$9.5_{1.1}$	—	—
Rainfall coefficient	β_{rain}	—	—	$0.008_{0.002}$	$0.08_{0.02}$
Temperature coefficient	β_{temp}	—	—	$-0.5_{0.6}$	$-0.06_{0.04}$
R over *T* coefficient	β_{ROT}	—	—	—	$-0.09_{0.01}$
Drug coefficient Quinine	β_{qui}	—	$2.2_{0.7}$	$0.45_{0.08}$	$0.39_{0.2}$
Drug coefficient Chloroquine	β_{clo}	—	$4.2_{0.8}$	$1.69_{0.01}$	$2.5_{0.3}$
Drug coefficient Fansidar	β_{fan}	—	$0.8_{0.7}$	$-0.4_{0.1}$	$-0.5_{0.2}$
Drug coefficient ACT	β_{act}	—	$0.9_{0.9}$	$-1.23_{0.09}$	$-1.8_{0.2}$
Spline coefficient	β_1	—	—	$0.46_{0.07}$	$0.5_{0.1}$
Spline coefficient	β_2	—	—	$-1.3_{0.1}$	$-1.6_{0.3}$
Spline coefficient	β_3	—	—	$-1.88_{0.03}$	$-1.9_{0.2}$
Spline coefficient	β_4	—	—	$0.5_{0.1}$	$1.1_{0.3}$
Spline coefficient	β_5	—	—	$2.0_{0.3}$	$3.2_{0.2}$
Spline coefficient	β_6	—	—	$0.3_{0.1}$	$0.8_{0.2}$

Number of fitted parameters, including initial conditions, and data points are listed. According to the second-order Akaike information criteria (AIC_c), the SpTR model better fits the observed data. Subscript numbers are the errors of the fitted parameters.